

Magnetization Characteristics Analysis in a Pole Changing Memory Motor Using Coupled FEM and Preisach Modeling

Jung Ho Lee* and Seung Chul Lee

Department of Electrical Engineering, Hanbat National University, Daejeon 305-719, Korea

(Received 27 July 2011, Received in final form 27 September 2011, Accepted 28 September 2011)

This paper deals with the magnetic equivalent circuit modeling and permanent magnet (PM) performance evaluations of a pole changing memory motor (PCMM). We use a coupled transient finite element method (FEM) and Preisach modeling, which is presented to analyze the magnetic characteristics of the permanent magnets. The focus of this paper is on the evaluation of characteristics such as the magnetizing direction and the pole number of the machine under re- and de-magnetization conditions.

Keywords : FEM, preisach's modeling, pole changing memory motor, magnetic equivalent circuit

1. Introduction

Memory motors combine the flux controllability of a PM (permanent magnet) machine with the high power density of conventional electric machines [1, 2].

They utilize the flux concentration principle which allows the generation of air gap flux densities that are typical for high-efficiency machines. Memory motors can be built either as variable-flux or pole-changing machines. In both machine types, the magnetization of PMs can be simply varied by using a short current pulse, with no need for a permanent demagnetizing current as in a conventional internal PM machine operating in flux weakening mode.

The operation of a memory motor is based on its ability to use a small stator current to change the magnetization of its magnets. This study illustrates how the magnetization of rotor magnets can be continually varied by applying a short pulse of stator current.

Factors such as the direction and strength of the magnetization are important in evaluating the performance of the memory motor. Such characteristics depend upon the characteristics of the magnetic material and therefore require a numerical evaluation. The Preisach model is now generally accepted to be a powerful hysteresis model and is therefore intensively studied [3, 4].

In this paper, we introduce the magnetic equivalent

circuit modeling and parameter calculation method for the selection of fundamental design variables for a pole changing memory motor (PCMM). A coupled finite element analysis and Preisach modeling for a PCMM are presented and a characteristic analysis is performed in the situation of pole changing due to a short pulse current.

2. Principle of Operation of the PCMM

2.1. Principle of Operation of the PCMM

Fig. 1 shows the cross-sectional view of a pole-changing memory motor with 32 tangentially magnetized magnets. On the rotor side there are four magnets per pole, all of which are magnetized in the same direction.

The rotor wreath is built of PMs along with iron segments and is mechanically fixed to a nonmagnetic shaft. After the stator winding is reconnected into a six-

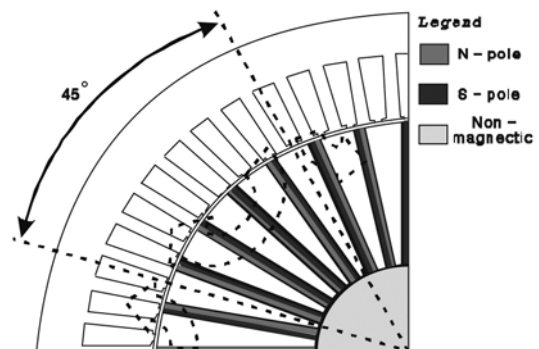


Fig. 1. 8-pole magnetized PCMM.

*Corresponding author: Tel: +82-42-821-1626

Fax: +82-42-821-1088, e-mail: limotor@hanbat.ac.kr

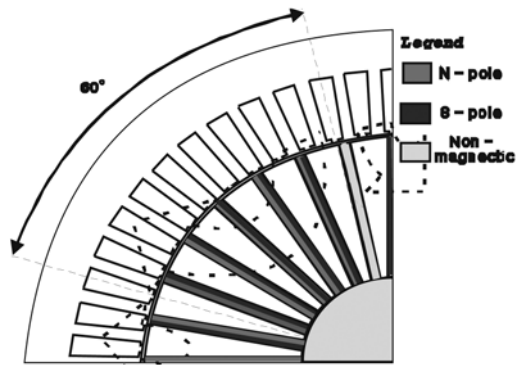


Fig. 2. 6-pole magnetized PCMM.

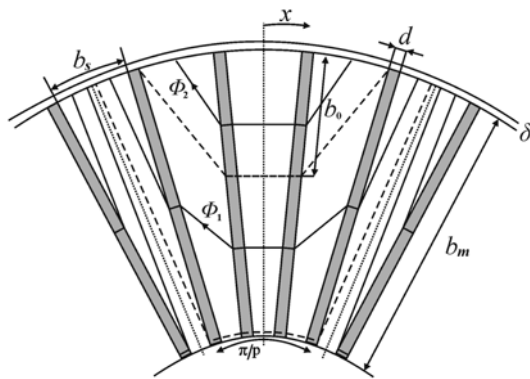


Fig. 3. Cross-sectional view of the PCMM with four magnets per pole.

pole configuration, a short pulse of stator current changes the rotor from eight-pole to six-pole magnetization, as shown in Fig. 2.

Since the number of magnets per pole is no longer an integer ($32/6=5.333\dots$), some magnets can remain demagnetized.

2.2. Magnetic Equivalent Circuit and Determination of Air Gap Flux Density

Assume that the rotor is built with 4 magnets per pole, and that all magnets are magnetized. The approximate flux density distribution in this case is shown in Fig. 3.

The flux Φ_1 in Fig. 3 goes through the whole area of the left and right magnets, but only through a portion of the center magnet with radial height $b_m - b_0$. The flux Φ_2 in Fig. 3 goes only through a portion of the center magnet with radial height b_0 .

Since the magnets are tangentially magnetized, and there is no current in the rotor slots, one may write the tangential component of rotor slot flux density as.

Denoting by B_r the residual magnetism of the rotor magnets, and their coercive force by H_c , one can define the quantities of the magnetic equivalent circuit in Fig. 4

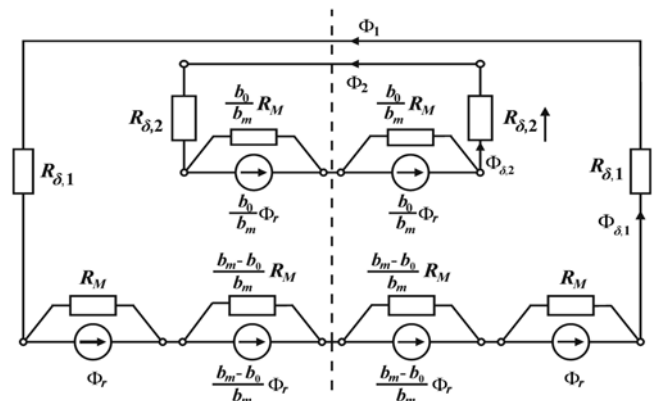


Fig. 4. Magnetic equivalent circuit of proposed model.

as:

$$G_M = \frac{B_r \ell \cdot b_m}{H_c d}, \quad G'_M = \frac{B_r \cdot \ell \cdot (b_m - b_0)}{H_c \cdot d}, \quad G''_M = \frac{B_r \cdot \ell \cdot b_0}{H_c \cdot d} \quad (1)$$

$$R_{\delta,1} = \frac{1}{\mu_0} \frac{\delta}{lb_s/2}, \quad R_{\delta,2} = \frac{1}{\mu_0} \frac{\delta}{lb_s}, \quad B(r) = \text{const.} \quad (2)$$

$$\phi_{\delta,1} = \frac{1}{1 + \left\{ G_M R_{\delta,1} \left(2 - \frac{b_0}{b_m} \right) \right\}} \cdot \phi_r, \quad \phi_{\delta,2} = \frac{1}{1 + G_M \left(\frac{b_0}{b_m} \right) R_{\delta,2}} \cdot \phi_r$$

$$\phi_1 = 2 \cdot \phi_{\delta,1}, \quad \phi_2 = 2 \cdot \phi_{\delta,2} \quad (3)$$

$$B_{\delta,1} = \frac{\mu_0 B_r}{\left\{ \left(\frac{\delta}{2d} \right) \left(\frac{B_r}{H_c} \right) + \mu_0 \left(\frac{b_s}{2b_m} \right) \right\}} + \frac{(b_m - b_0) \mu_0 B_r}{\left\{ \left(\frac{\delta}{2d} \right) \left(\frac{B_r}{H_c} \right) + \mu_0 \left(\frac{b_s}{2(b_m - b_0)} \right) \right\}}$$

$$B_{\delta,2} = \frac{\mu_0 B_r}{\left\{ \left(\frac{\delta}{2d} \right) \left(\frac{B_r}{H_c} \right) + \mu_0 \left(\frac{b_s}{2b_0} \right) \right\}} \quad (4)$$

where, G_M ; magnetic reluctance

$R_{\delta,1}, R_{\delta,2}$; air gap reluctance

$F_{\delta,1}, F_{\delta,2}$; air gap flux

$B_{\delta,1}, B_{\delta,2}$; air gap flux density.

The solution for fluxes Φ_1 and Φ_2 in Fig. 4 helps one to find the flux per pole, Φ_{pole} , as a function of magnet residual flux Φ_r as

$$\frac{\phi_{pole}}{\phi_r} = 2 \times \left\{ \frac{\frac{7}{2}y + 2}{\frac{3}{2}y^2 + \frac{7}{2}y + 1} \right\}, \quad (5)$$

with y denoting the ratio between the reluctances of the air gap and the magnet,

$$y = \frac{R_{\delta,2}}{R_M} = R_{\delta,2} G_M. \quad (6)$$

An increase in the thickness d of the magnets results in

higher air gap flux densities $B_{\delta 1}$ and $B_{\delta 2}$ compared to the residual flux density B_r (0.4 T).

2.3. De/Remagnetization Ampere-turns

The number of stator ampere-turns which de- or remagnetizes the rotor magnets is found by applying Ampere's circuital law for the loops concatenating the stator current sheet and passing through the rotor magnets [2].

Two such loops are shown in Fig. 3, with arrows denoting the direction of fluxes Φ_1 and Φ_2 . Using the index a for magnetic quantities in the two central slots, b for those in the two side slots, and δ for the air gap, one can write for the integration loop of Φ_2 ,

$$\oint H \cdot d\ell = H_\delta \delta + H_a d = Ax, \quad (7)$$

with A representing the amplitude of the current sheet created by stator winding. The above equation helps one to find the flux Φ_2 as

$$\phi_2 = \frac{\mu_0 \ell}{\delta} (b_s - d)(Ab_s - H_a d) \quad (8)$$

Substituting for magnetomotive force (MMF) drop on the center slot the product of flux Φ_2 and slot reluctance, one obtains for the field strength H_a in the center slot:

$$H_a = \frac{b_s (b_s - d)}{\delta b_0 + d (b_s - d)} A. \quad (9)$$

Similarly, for the integration loop with flux Φ_1

$$\oint H \cdot d\ell = H_\delta \delta + H_a d + H_b d = Ax, \quad (10)$$

$$\phi_1 = \frac{\mu_0 \ell}{2\delta} (b_s - d) \left(\frac{7b_s + d}{4} A - dH_a - dH_b \right), \quad (11)$$

$$\left(2\delta \frac{b_m - b_0}{b_s - d} + d \right) H_a + dH_b = \frac{7b_s + d}{4} A \quad (12)$$

and

$$\left(2\delta \frac{b_m}{b_s - d} + d \right) H_b + dH_a = \frac{7b_s + d}{4} A. \quad (13)$$

Simultaneous solution of the three above equations gives the values of b_0 , H_a and H_b as a function of the machine geometry and the amplitude of stator current sheet A [5, 6].

For a discrete distribution of currents in the slots, the current sheet is given by

$$A = \frac{I_s}{o}, \quad i_{de} = \frac{I_s}{2 \cdot TN}, \quad (14)$$

where I_s is the total current per slot, i.e. the sum of the currents in all of the conductors in a slot, o is the size of the slot opening, i_{de} is the input de- or remagnetizing

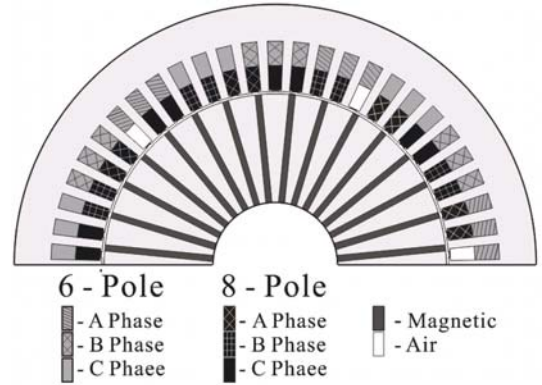


Fig. 5. (Color online) slot winding (6/8 pole) and material.

current, and TN is the number of turns.

3. Coupled FEM and Preisach's Modeling

3.1. Governing Equation of PCMM

Maxwell's equations can be written as

$$\nabla \times \vec{H} = \vec{J}_0 \quad (15)$$

$$\nabla \cdot \vec{B} = 0 \quad (16)$$

$$\vec{B} = \frac{1}{\nu_0} \vec{H} + \vec{M} \quad \vec{B} = \frac{1}{\nu_0} \vec{H} + \vec{M}_{PM} \quad (17)$$

where \vec{M} and \vec{M}_{PM} are the magnetizations of the magnetic material and the permanent magnet with respect to the magnetic intensity \vec{H} . The magnetic vector potential \vec{A} and the equivalent magnetizing currents \vec{J}_m and \vec{J}_{PMm} are expressed as follows:

$$\vec{B} = \nabla \times \vec{A} \quad (18)$$

$$\vec{J}_m = \nu_0 (\nabla \times \vec{M}), \quad \vec{J}_{PMm} = \nu_0 (\nabla \times \vec{M}_{PM}). \quad (19)$$

The governing equation derived from (15)-(19) is given by

$$\nu_0 (\nabla \times \nabla \times \vec{A}) = \vec{J}_0 + \vec{J}_m + \vec{J}_{PMm}. \quad (20)$$

3.2. System Matrix Static Analysis

The overall model is described by the following matrix:

$$[K]\{A\} + \{F\} + \{M\} + \{M_{PM}\} = 0. \quad (21)$$

3.3. Application of Preisach's Model

The magnetization M can be described by a scalar model, because the rotor rotates synchronously with the input current angle θ . Therefore, it can be supposed that the magnetic domain in the stator is an alternating field with reference to the x and y axes. The B and H of the domain in the rotor are constant and the domain is a rotating field, which is also an alternating field with

reference to the x and y axes [4]. It is natural that M and H, which are calculated with reference to the same axes, have the same vector direction:

$$M(t) = \iint_{\alpha \geq \beta} \mu(\alpha, \beta) \gamma_{\alpha\beta}(H(t)) d\alpha d\beta \quad (22)$$

$$= \iint_{S^+(t)} \mu(\alpha, \beta) d\alpha d\beta - \iint_{S^-(t)} \mu(\alpha, \beta) d\alpha d\beta$$

A more convenient treatment of this model is to substitute the Everett plane for Preisach's one as shown in Eq. (23):

$$E(\alpha, \beta) = \iint_{\alpha \geq \beta} \mu(\alpha, \beta) \gamma_{\alpha\beta}(H(t)) d\alpha d\beta \quad (23)$$

In the Everett plane, the distributions of M calculated assuming the experimental data of the material S40 and the ferrite magnet (0.4 T, Coercive force: 250×10^4 A/m) are Gaussian.

4. Algorithm of Computing

4.1. Computing Algorithm

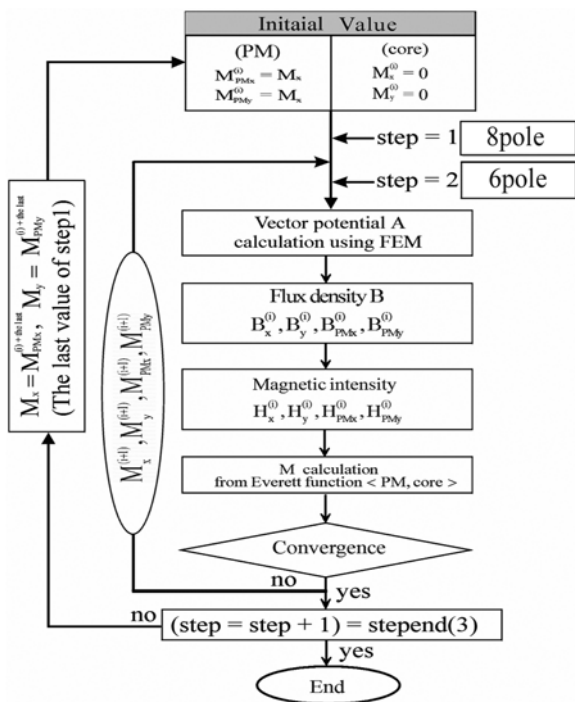


Fig. 6. Flow chart of FEM using Preisach's model.

5. Results and Discussion

The input de/remagnetizing currents are calculated by Eq. (9) and Eq. (12)-(14).

Table 1 shows the de/remagnetizing currents for various magnet thicknesses. As can be seen in Table 1, more stator current is needed to de- or remagnetize the rotor

Table 1. De/Remagnetizing currents according to the magnet thickness

Magnet thickness (mm)	Current (A)
6	6.13
7	7.33
8	8.16
9	9.86
10	10.83
11	12.14
12	13.53
13	14.95
14	16.31

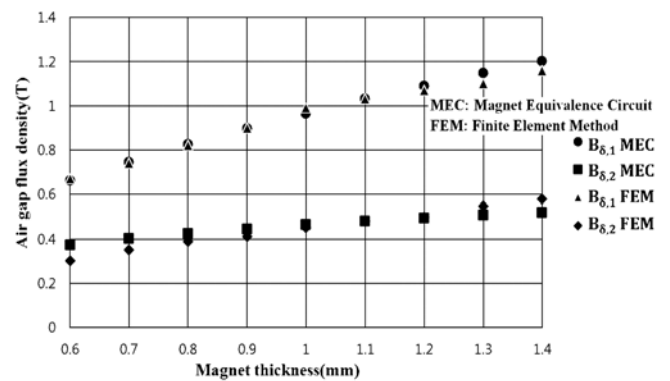


Fig. 7. Air gap flux density according to magnet thickness variations of the proposed model.

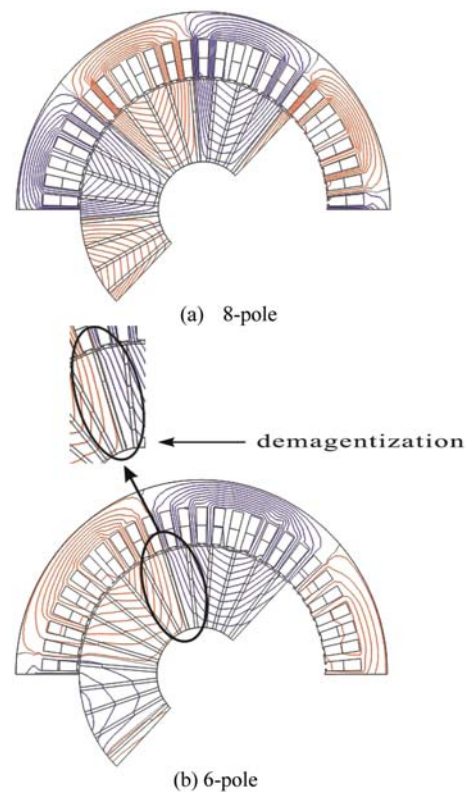


Fig. 8. (Color online) 8 pole and 6 pole Flux plots of PCMM.

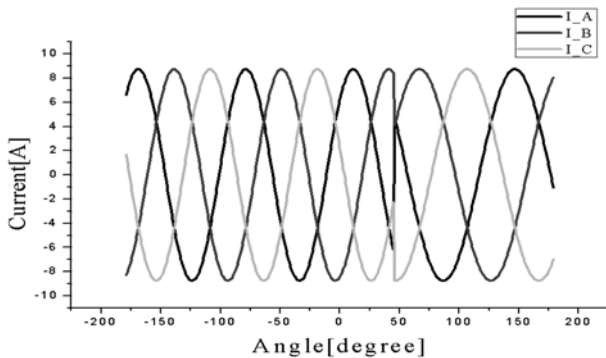


Fig. 9. Input current of PCMM in 8 pole/6 pole drive.

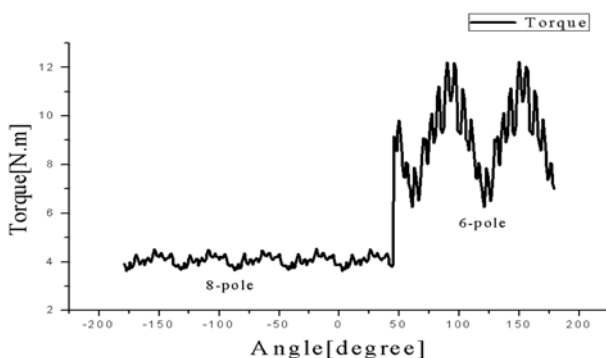


Fig. 10. Torque response (8 pole/6 pole).

magnets when the thickness of the magnets increases. There obviously exists an optimum thickness of magnets per pole at which the de/remagnetization current is not too much bigger than the rated one.

Fig. 7 shows the air gap flux densities $B_{\delta 1}$ and $B_{\delta 2}$ calculated using the proposed magnetic equivalent circuit according to magnet thickness variations in the model of this paper. As shown in Fig. 7, it is confirmed that the results are closely matched to those of the coupled FEM & Preisach model.

After the stator winding is reconnected into the six-pole configuration, a short pulse of stator current (magnet thickness: 1 mm) changes the rotor from the eight-pole magnetization to a six-pole one, as shown in Fig. 8.

Since the number of magnets per pole is no longer an integer ($32/6 = 5.333\dots$), a magnet can remain demagnetized, as shown in Fig. 8.

Fig. 9 show the input currents during 8/6 pole drive at a constant power. The input current is switched at an angle of 45 degrees, from 8 pole to 6 pole.

Whereas the frequency of 6-pole drive is slower than that of 8-pole, as can be seen in Fig. 9, the torque of 6-

pole drive is larger than that of 8-pole because the driving power is constant, as shown in Fig. 10.

6. Conclusion

In this paper, we introduce the magnetic equivalent circuit modeling and parameter calculation method for the selection of fundamental design variables for a Pole Changing Memory Motor (PCMM). In addition, the input de/remagnetizing currents for the 8/6 pole switching are selected.

In order to prove the above modeling and method, a magnetizing characteristic analysis method has been proposed, which is suited to the evaluation of machines with magnetic non-linearity, hysteresis phenomena and magnetizations.

The direction and strength of the magnetization of a pole changing memory motor (PCMM) according to a stator MMF with 8/6 poles are investigated. With this procedure, it is possible to investigate the influence of short pulse stator current components on the overall magnetization from an 8-pole to a 6-pole configuration.

It should be noted that the fundamental design solutions of a PCMM are related to the rotor magnet dimensions and the stator MMF, which are important factors in a PCMM design.

Acknowledgment

This research was supported by Basic Science Research Program through the National Research Foundation of Korea (NRF) funded by the Ministry of Education, Science and Technology (grant 2010-0005711).

References

- [1] V. Ostovic, in Conf. Rec. IEEE - IAS Annu. Meeting, 2577 (2001).
- [2] V. Ostovic, IEEE Trans. Ind. Appl. **38**, 1493 (2002).
- [3] A. Ivanyi, Hysteresis Models in Electromagnetic Computation, Akademiai Kiado, Budapest (1997).
- [4] J. H. Lee, J. C. Kim, and D. S. Hyun, IEEE Trans. Magn. **34**, 2629 (1998).
- [5] V. Ostovic, Dynamics of Saturated Electric Machines, Springer Verlag, New York (1989).
- [6] V. Ostovic, Computer-Aided Analysis of Electric Machines - A Mathematica Approach, Prentice-Hall, Englewood Cliffs (1994).